catalysts

MDPI

Article

Integrated CO_2 Capture and Hydrogenation to Produce Formate in Aqueous Amine Solutions Using Pd-Based Catalyst

Lichun Li [1,2,*], Xiangcan Chen [2], Chu Yao [2] and Meng Xu [2,*]

[1] Research Center for Environmental and Energy Catalysis, Institute of Fundamental and Frontier Sciences, University of Electronic Science and Technology of China, Chengdu 611731, China
[2] College of Chemical Engineering, Zhejiang University of Technology, 18 Chaowang Road, Hangzhou 310014, China
* Correspondence: lichunli@zjut.edu.cn (L.L.); xumeng@zjut.edu.cn (M.X.)

Abstract: Integrated CO_2 capture and hydrogenation to produce formate offers a sustainable approach for reducing carbon dioxide emissions and producing liquid hydrogen carriers (formate) simultaneously. In the current study, three different types of aqueous amine solutions including monoethanolamine (MEA), diethanolamine (DEA) and triethanolamine (TEA) were investigated as CO_2-capturing and hydrogenation agents in the presence of a Pd/NAC catalyst. The effect of amine structures on the CO_2 absorption products and formate yield was investigated thoroughly. It was found that the formate product was successfully produced in the presence of all three aqueous amine solutions, with tertiary amine TEA accounting for the highest formate yield under the same CO_2 loadings. This is due to the fact that primary and secondary amine moieties in MEA and DEA are responsible for the formation of CO_2 adducts of carbamate and bicarbonate, whereas the tertiary amine moiety in TEA is responsible for the formation of hydrogenation-favorable bicarbonate as the solo CO_2 absorption product. A high yield of formate of 82.6% was achieved when hydrogenating 3 M TEA with 0.3 mol CO_2/mol amine solution in the presence of a Pd/NAC catalyst. In addition, the physio-chemical properties of the Pd/NAC catalyst analyzed using TEM, XRD and XPS characterization were applied to rationalize the superior catalytic performance of the catalyst. The reaction mechanism of integrated CO_2 capture and hydrogenation to produce formate in aqueous amine solutions over Pd/NAC catalyst was proposed as well.

Keywords: CO_2 capture; CO_2 hydrogenation; heterogenous catalysts; Pd catalyst; formate

Citation: Li, L.; Chen, X.; Yao, C.; Xu, M. Integrated CO_2 Capture and Hydrogenation to Produce Formate in Aqueous Amine Solutions Using Pd-Based Catalyst. *Catalysts* **2022**, *12*, 925. https://doi.org/10.3390/catal12080925

Academic Editor: Consuelo Alvarez-Galvan

Received: 13 July 2022
Accepted: 18 August 2022
Published: 21 August 2022

1. Introduction

The excessive emissions of CO_2 are regarded as a main cause for global warming, while CO_2 capture technologies and exploring clean energy replacement are the two main strategies to reduce CO_2 emissions [1–4]. CO_2 capture and utilization technology (CCU) has been widely investigated in recent years as it offers an effective way to mitigate CO_2 emissions and tackle the global warming issue [5,6]. For the traditional decoupled CCU process, CO_2 was firstly captured from fossil fuel burning points and industrial sources. The obtained pure CO_2 was then pressurized and transported to specified locations for CO_2 utilization. For a typical CO_2 capture process, CO_2 was firstly adsorbed at low temperature (40~60 °C) via exothermal chemical interaction with aqueous amine solvents, then desorbed at high temperature (100~150 °C) through an endothermic process to generate pure CO_2. The energy-intensive CO_2 desorption process is regarded as one of the main issues blocking the commercialization process of CO_2 capture process [7]. With the assistance of a suitable catalyst, the aqueous-amine-captured CO_2 can be directly hydrogenated into value-added products, which can eliminate the energy-intensive CO_2 desorption step and result in an energy-efficient integrated CO_2 capture and hydrogenation process [8].

Integrated CO_2 capture and hydrogenation to produce formate process offers a sustainable approach to reduce CO_2 emissions and produce liquid hydrogen carriers at the same

time. When heating up the obtained ammonium formate solution, formic acid product can be generated from thermal cleavage, which is accompanied by the regeneration of aqueous amine solvents. The concept of integrated CO_2 capture and hydrogenation to produce formate was firstly reported by He et al. in 2013 [9]. They reported the successful application of CO_2 absorption into polyethyleneimine 600 (PEI600) sorbents in methanol and in situ hydrogenation to produce alkylammonium formate with the assistance of homogeneous catalyst $RhCl_3.3H_2O/CyPPh_2$. The authors demonstrated a highest turnover number of 726, corresponding to a 55% formate yield under the reaction conditions of 40 bar H_2, 60 °C and a reaction time of 16 h. Later, the integrated CO_2 capture and hydrogenation process was extended to aqueous amine solutions as CO_2 capture in such solvents is most widely explored and suitable for scale-up. In 2014, Hicks et al. reported the application of a polyethyleneimine-tethered iminophosphine iridium catalyst for integrated CO_2 capture and hydrogenation to produce formate in triethylamine solutions, with a TON of 248 achieved under reaction conditions of 20 bar H_2 and 120 °C [10]. An outstanding high TON value of 7375 was reported by Olah and Prakash et al. upon integrated CO_2 capture and hydrogenation in TMG solutions with Ru-Macgo-BH as a homogeneous catalyst [11]. In the same paper, an iron-based homogeneous catalyst was also explored as a promising candidate for CO_2 capture and hydrogenation in pentaethylenehexamine (PEHA) solutions with a TON of 255 obtained. Although the application of homogeneous catalysts in the CO_2 capture and hydrogenation process to produce formate demonstrated superior catalytic performance with high formate yields and TON values, the common issues related to homogeneous catalysts including the recycling of catalysts and the separation of products still hindered the scale-up of such a process. On the other hand, integrated CO_2 capture and hydrogenation to produce formate in aqueous amine solution using Pd-based catalysts is rarely reported in the open literature. One such example is reported by Lin's group, who stated that they successfully produced formate with a product yield of 50.2% using piperidine as a CO_2-capturing solvent and Pd/AC as a catalyst [12]. However, the effect of amine structure on the product yield was not reported in the open literature.

In the current study, three different aqueous amine solutions with different amine types including primary amine monoethanolamine (MEA), secondary amine diethanolamine (DEA) and triethanolamine (TEA) were employed as CO_2-capturing and hydrogenation solvents in the presence of Pd/NAC catalysts. The CO_2 absorption product distribution together with formate yield at different CO_2 loadings were measured and compared between the three different aqueous amine solutions. XRD, XPS and TEM were employed to evaluate the physio-chemical properties of the Pd/NAC catalysts in order to rationalize the corresponding catalytic performance. At last, the reaction mechanism of integrated CO_2 capture and hydrogenation in the presence of the Pd/NAC catalyst was proposed.

2. Results and Discussion

2.1. Integrated CO_2 Capture and Hydrogenation to Produce Formate

Pd-based supported heterogeneous catalysts have demonstrated superior catalytic performance towards the hydrogenation of HCO_3^- in aqueous phase compared with other metal catalysts of Ni, Ru, Co and Re [13]. Carbon-based materials were widely applied as supporting materials for Pd-based heterogeneous catalysts for their application in the hydrogenation of HCO_3^- in aqueous phase [13–18], among which, the generation of N-containing functional groups from synthesizing a particular type of carbon-based material, including nitrogen-doped carbon (NMC) and graphitic carbon nitride (g-C_3N_4), is well-accepted as an efficient way to manipulate the interaction between a support and active metal Pd. N-containing surface groups are often recognized as electron-donating functionalities which is beneficial to anchor and increase the electron density of active metal Pd. Therefore, a nitrogen-doped activated carbon (NAC)-supported Pd catalyst was employed as the heterogeneous catalyst for the integrated CO_2 capture and hydrogenation process. The NAC material used herein was prepared via a simple solid mixing and thermal treatment procedure.

To investigate the effect of amine structure on the product yield, three aqueous amine solutions including MEA, DEA and TEA were employed as capturing agents for the integrated CO_2 capture and hydrogenation process. The results of integrated CO_2 capture and hydrogenation in aqueous amine solutions of MEA, DEA and TEA in the presence of a Pd/NAC catalyst are shown in Table 1. In addition, we performed the integrated CO_2 capture and hydrogenation process with 3M TEA solutions, 0.30 mol CO2/mol amine, with NAC as the catalyst, and the NMR results showed no characterization peak for formate was formed after the reaction.

Table 1. Results of integrated CO_2 capture and hydrogenation to produce formate in aqueous amine solutions of MEA, DEA and TEA in the presence of Pd/NAC catalyst.

Entry	Capturing and Hydrogenation Solvent	CO_2 Loading	Captured CO_2 Concentration (M)		Hydrogenation Results of CO_2 Species Concentration (M)			Conversion Results
			HCO_3^-	$R_1R_2COO^-$	HCO_3^-	$R_1R_2COO^-$	$HCOO^-$	Formate Yield (%)
1	MEA	0.15	0	0.45	0	0.31	0.14	30.8
2	MEA	0.31	0.14	0.79	0	0.55	0.38	40.8
3	MEA	0.46	0.25	1.13	0	0.63	0.75	54.1
4	MEA	0.72	1.19	0.97	0	0.89	1.27	58.8
5	DEA	0.16	0	0.48	0	0.29	0.19	35.1
6	DEA	0.31	0.17	0.76	0	0.5	0.43	50.3
7	DEA	0.48	0.45	0.98	0	0.71	0.72	46.3
8	DEA	0.78	0.70	1.64	0	1.16	1.18	60.6
9	TEA	0.15	0.45	0	0.14	0	0.31	68.5
10	TEA	0.30	0.9	0	0.16	0	0.74	82.6
11	TEA	0.46	1.38	0	0.51	0	0.86	62.5
12	TEA	0.60	1.8	0	0.84	0	0.96	53.2

Reaction conditions: 80 °C, 5.0 mL 3M amine solutions, 6 MPa H_2, 100 mg catalyst and reacting time of 8 h.

As expected, the CO_2-capturing product in MEA and DEA solutions contained both bicarbonate (HCO_3^-) and carbamate ($R_1R_2COO^-$) species, as CO_2 can directly react with primary/secondary amines. Meanwhile, HCO_3^- was the solo CO_2 absorption product for TEA, since CO_2 cannot react directly with tertiary amine groups. It is interesting to find that the concentrations of HCO_3^- species appeared to be 0 after the integrated CO_2 capture and hydrogenation process in both the MEA and DEA solutions, meaning that all HCO_3^- species were converted into formate products. However, there were still some carbamate species left in the liquid phase after the hydrogenation process. This interesting phenomenon proves that HCO_3^- is a more favorable reactant for the hydrogenation process compared with the carbamate species. This agrees well with results published in the literature that show HCO_3^- can act directly as a reactant for the hydrogenation process; however, the direct conversion of carbamate is rather difficult due to its electron-rich nature [19]. The conversion of carbamate species can be achieved via two possible pathways including 1) the conversion of carbamate into bicarbonate then participating in the hydrogenation process, and 2) the conversion of carbamate species into gaseous CO_2 under the reaction temperature of 80 °C then participating in the hydrogenation process. However, the low solubility of CO_2 under reaction conditions makes the second pathway less possible. Therefore, the hydrogenation of carbamate species is assumed to be through the HCO_3^- pathway.

Compared with MEA and DEA, TEA often demonstrated the highest formate yield under the same CO_2 loadings. For example, at the CO_2 loading of ~0.3, a formate yield of 82.6% was achieved when employing TEA as the CO_2-capturing and hydrogenating solvent, while formate yields of only 40.8% and 50.3% were achieved when employing MEA and DEA as CO_2-capturing and hydrogenating solvents. The fact that a higher formate yield was often achieved in TEA solutions under the same CO_2 loading was attributed to

the favorable hydrogenation when HCO_3^- species were the solo CO_2-capturing adducts in the TEA solutions.

Among all tested amine solutions with different CO_2 loadings, the highest formate yield of 82.6% was achieved when using TEA as the CO_2-capturing and hydrogenation agent with CO_2 loading of 0.30 mol CO_2/mol amine. For the TEA solution, the concentration of formate product increased with the increase in CO_2 loading. However, the formate yield increased with CO_2 loading when CO_2 loading was below 0.3 mol CO_2/mol amine and decreased with the increase in CO_2 loading when CO_2 loading was above 0.3 mol CO_2/mol amine.

2.2. Catalyst Characterization

To rationalize the catalytic performance with the physical–chemistry properties of the Pd/NAC catalyst and propose the reaction mechanism, XRD, XPS and TEM measurements were performed on the catalyst. The XRD pattern of the Pd/NAC catalyst is shown in Figure 1. The diffraction peaks at 2θ of 40.1°, 46.7° and 68.1° corresponded to the (111), (200) and (220) crystalline planes of Pd (PDF# 46-1043). This certainly indicates the existence of crystalline Pd in zero valance (Pd^0), which is well-believed to be the active site for the dissociative adsorption of H_2 in heterogeneous hydrogenation processes.

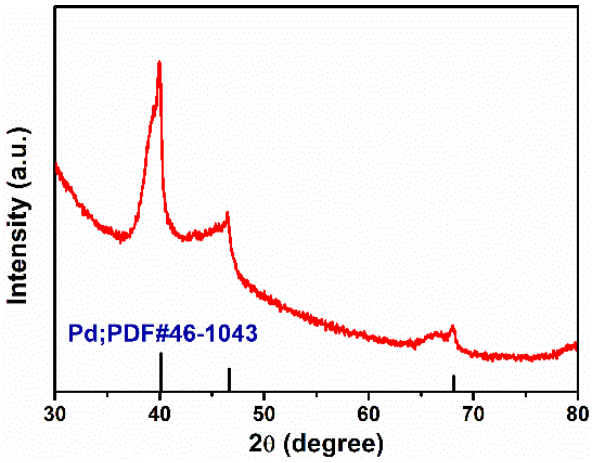

Figure 1. XRD pattern of the Pd/NAC catalyst.

Particle size is often believed to be one of the crucial features governing the catalytic performance of supported metal catalysts in heterogeneous reactions [20,21]. For example, the optimized Pd nanoparticle size appeared to be within the range of 1.8–3.5 nm in an aqueous phase formic acid dehydrogenation reaction process. For the hydrogenation of bicarbonate in aqueous solutions, the reported mean particle size of Pd nanoparticles with decent catalytic activity falls in the range of 1.6 to 3.1 nm. Cao et al. reported the application of a 5 wt% Pd/r-GO catalyst with a mean particle size of 2.4 nm for the hydrogenation of 4.8 M $KHCO_3$ solution under conditions of 100 °C and 40 bar H_2; a formate yield of 66.3% was obtained after 10 h of reaction [16]. Zhang et al. investigated the application of Pd/AC and Pd/MNC catalysts in a system of the hydrogenation of 4 M $KHCO_3$ solutions at 353 K [17]. A high formate yield of 69.7% was obtained after a reaction time of 2 h in the presence of the Pd/MCN catalyst with a mean particle size of 2.4 nm, while a low formate yield of 43.2% was obtained after a reaction time of 3 h in the presence of the Pd/AC catalyst with a particle size of 3.1 nm. Therefore, the TEM technique was employed to obtain information on nanoparticle size in the Pd/NAC catalyst. The measured TEM image and corresponding particle size distribution plot of the Pd/NAC catalyst are presented in Figure 2a,b.

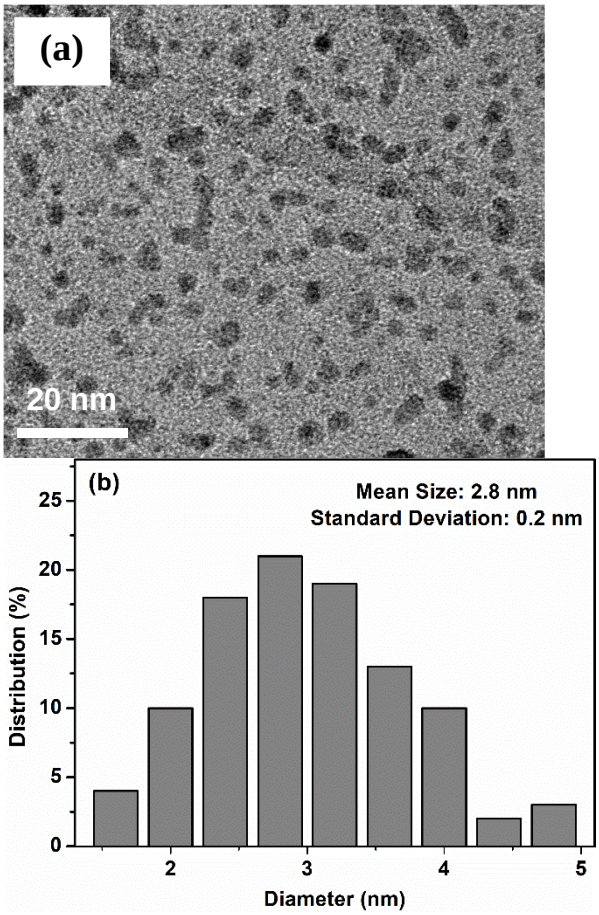

Figure 2. TEM image (**a**) and corresponding particle distribution plot (**b**) of Pd/NAC catalyst.

As can be seen from Figure 2a, the Pd nanoparticles were uniformly distributed on the NAC catalyst. The mean sizes and standard deviations of the Pd nanoparticles were calculated using 100 individual nanoparticles. The calculated average diameter of the Pd nanoparticles was 2.8 ± 0.2 nm. The obtained mean particle size of Pd nanoparticles on the Pd/NAC catalyst fell into the decent-activity nanoparticle size range of 1.6 to 3.1 nm, which was likely to facilitate the hydrogenation of HCO_3^- in the integrated reaction process.

The XPS technique is a useful tool to examine the valence states and surface composition of metal-based catalysts [22–24]. Therefore, to further acquire information on the chemical state of Pd and surface N-containing groups, XPS measurement was performed for the Pd/NAC catalyst. The XPS spectra of Pd 3d and N 1s core level of Pd/NAC catalyst were measured and are presented in Figure 3a,b.

There are two main doublets that could be observed in the deconvoluted XPS spectra of the Pd 3d region (Figure 3a), which indicates the existence of two different Pd chemical states of Pd^0 and Pd^{2+}. The two intense doublets observed at 336.2 and 341.5 eV were attributed to the characteristic peaks of metallic Pd (Pd^0). The other residual weak peaks at 338.0 and 343.3 eV were attributed to the characteristic peaks of Pd^{2+}. By integrating the corresponding peak areas for the Pd^0 and Pd^{2+}, the ratio between surface Pd^0 and Pd^{2+} appeared to be 71.4:28.6. This result suggests the formation of a large amount of metallic Pd on the surface of the Pd/NAC catalyst, which is assumed to be the active site for H_2 adsorption and dissociation. The amount of metallic Pd is highly related to the reactivity of the hydrogenation reaction; hence, a potential increase in the hydrogenation reactivity can be achieved via further increase in the Pd^0 amount on the surface of the catalyst. As can be seen in Figure 3 (b), four types of N-containing functionalities were identified on the surface of the Pd/NAC catalyst containing pyridine (N1, 398.7 eV), nitrile (N2, 399.3 eV), pyrrole (N3, 400.3 eV) and quaternary N (N4,400.9 eV) [25,26]. As

reported by Lee et al., the sp^2 nitrogen site appears to have more diffuse orbitals and more negative charges, which are likely to interact with the Pd^{2+} in the precursor and benefit the reduction of Pd^{2+} into Pd^0 in a subsequent reducing procedure [27]. The abundant amount of surface N-containing groups are believed to be electron-donating functionalities which can increase the electron density of Pd^0 on the surface of the Pd/NAC catalyst. The electron-enriched Pd nanoparticle was often accompanied with decent catalytic activity in the hydrogenation of bicarbonate; therefore, decent catalytic performance was observed when using the Pd/NAC catalyst for the hydrogenation of CO_2-captured amine solutions. The used catalyst was collected following a filtration, water wash and dry process in order to examine the chemical state of Pd after the reaction. The XPS spectra of the Pd 3d core level of the used Pd/NAC catalyst can be found in Figure S1 of the Supporting Information, demonstrating a minor change in the chemical state of Pd on the surface of the catalyst with a similar Pd^0 and Pd^{2+} ratio compared with the fresh catalyst.

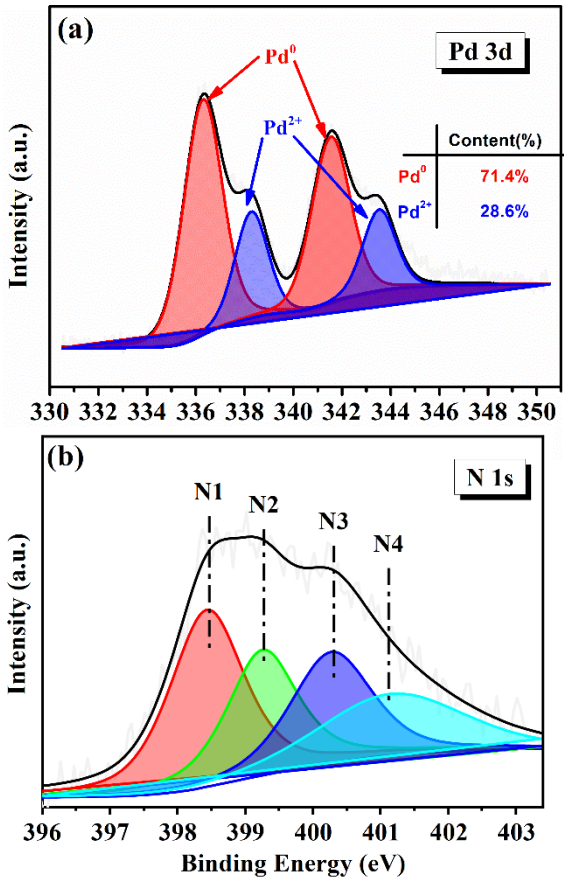

Figure 3. XPS spectra of Pd 3d (**a**) and N 1s (**b**) core level of Pd/NAC catalyst.

2.3. Reaction Mechanism

Based on the understanding of Pd nanoparticle size and its corresponding chemical state on the surface of the Pd/NAC catalyst, the reaction mechanism of the integrated CO_2 capture and in situ hydrogenation to produce formate in aqueous amine solutions with Pd/NAC catalyst was proposed and is illustrated in Figure 4. Firstly, CO_2 was adsorbed into aqueous amine solutions with $R_1R_2NCOO^-$ and HCO_3^- as the main CO_2-capturing products in primary/secondary amine solutions and HCO_3^- as the solo main CO_2-capturing product in tertiary amine solutions. Secondly, HCO_3^- was acting as the main hydrogenation reactant in all amine solutions, while the carbamate species $R_1R_2NCOO^-$ was transformed into the form of HCO_3^- through an equilibrium reaction before participating in the hydrogenation process. The following procedure was the hydrogenation of bicarbonate into a formate product, which follows the insertion mechanism as

reported in the open literature [17,28]. As indicated from the XPS results, the Pd nanoparticles were in the electron-enriched state, which was beneficial for the following HCO_3^- hydrogenation process. The residual free amine molecules in the solutions were also recognized as electron-donating species, which would increase the electron-enriched state of Pd and benefit the subsequent hydrogenation process. Basically, the HCO_3^- species was adsorbed on the surface of the NAC support and H_2 was adsorbed and activated on the Pd site to form surface Pd-H species. The Pd-H species then attacked the positively polarized carbon in HCO_3^- to form formate product. Lastly, the formate product desorbed from the surface of the catalyst, followed by the regeneration of the fresh Pd/NAC catalyst for the adsorption and activation of HCO_3^- and H_2 reactants.

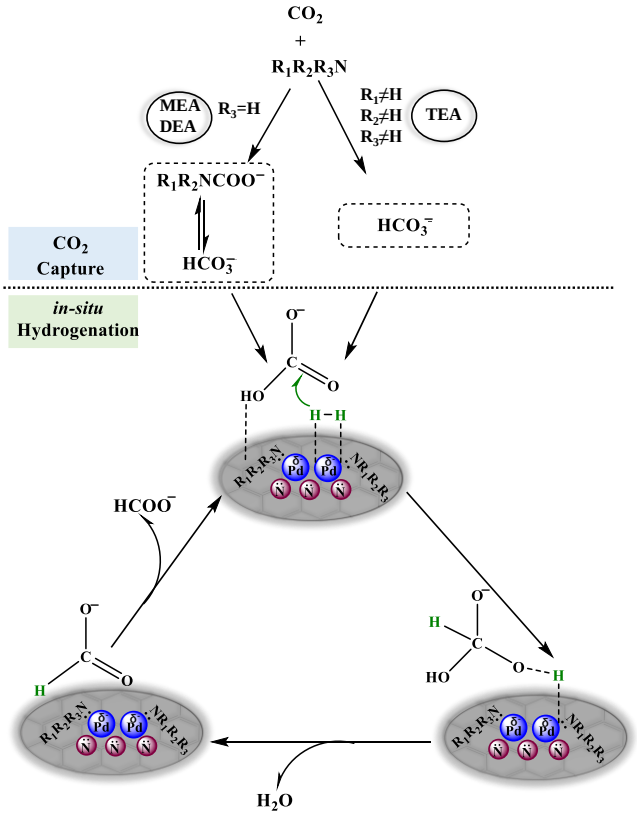

Figure 4. Scheme of reaction mechanism of integrated CO_2 capture and hydrogenation in aqueous amine solutions catalyzed by Pd/NAC.

3. Materials and Methods

Preparation of catalyst: The N-doped activated carbon (NAC) was prepared by a simple solid mixing and thermal treatment procedure using melamine as the nitrogen source. Activated carbon was initially washed with HCl solution (1 M, 500 mL) at 75 °C for 2 h. The obtained activated carbon was then filtered and washed with distilled water and dried at 110 °C for 12 h (sample AC). Then, 5 g of AC was mixed evenly with 5 g of melamine in a porcelain boat. Then, the mixture was calcined at 700 °C for 2 h at a heating rate of 3 °C·min^{-1}. There was no gas during the heating up process and the first 90 min of the keeping stage. In the last 30 min, N_2 was passed into the tube furnace with a flow of 30 mL·min^{-1}. The obtained N-doped AC sample was named NAC. An ultrasonic-assisted method was applied to deposit Pd on NAC, and the pretreated NAC was grinded to achieve a sample size less than 0.1 mm before the deposition. Then, 0.5 g NAC was suspended in 50 mL of deionized water, and the mixture was immersed into an ultrasonic instrument filled with water (by changing the water frequently to maintain the reaction temperature between 30 and 35 °C) for 30 min so that NAC could be dispersed to a uniform suspension. After that, 8.6 mL of $PdCl_2$ aqueous solution (2.9 mg/mL) was added into the N-doped

carbon suspension under ultrasonication, allowing the chelate adsorption of Pd^{2+} on NAC. After being ultrasonicated for 1 h, 25 mL of $NaBH_4$ aqueous solution (4 mg/mL) was added dropwise, and the resulting suspension was maintained under ultrasonication for 2 h to allow a complete reduction of metallic salt. The slurry at last was filtered, washed with deionized water several times and dried under vacuum at 70 °C overnight.

Integrated CO_2 capture and hydrogenation: The CO_2 capture process was performed at room temperature via bubbling CO_2 into 3 M amine solutions, and the CO_2 content in the solutions was weighted to determine the CO_2 loading. The CO_2 flow rate was controlled at 80 mL/min. The subsequent hydrogenation was carried out in a high-pressure micro reactor. Typically, 5.0 mL of CO_2-loaded amine solution and Pd/NAC catalyst was placed in the reactor. Then, the reactor was sealed, and H_2 gas was charged after the internal air was scrubbed completely by using H_2 at room temperature. The stirrer (1000 rpm) was started until the desired reaction temperature of 80 °C was reached. After a certain reaction time, the reactor was placed in cool water, and the gas was carefully released. Afterwards, the reaction mixture was centrifuged to collect liquid products. The liquid products were then measured using ^{13}NMR.

The formate yield was calculated via the concentration of formate product divided by the concentration of total captured CO_2 concentration.

$$\text{Yield} = \frac{\text{mole of formate product}}{\text{mole of amine Captured } CO_2} \times 100\% \quad (1)$$

Catalyst characterization: The JEOL JEM-1200EX electron microscope operated at 200 kV was applied to measure the transmission electron microscopy (TEM) images of the Pd/NAC catalyst. In order to increase the conductivity, the catalyst was gold-plated before acquiring the TEM images. X-ray photoelectron spectroscopy (XPS) measurements were obtained on an ESCALAB 250XI spectrometer with 24.2 W of Al Kα radiation.

4. Conclusions

In the current paper, three aqueous amine solutions were evaluated as CO_2-capturing and hydrogenating agents and successfully produced formate product in the presence of a Pd/NAC catalyst. Among the three tested aqueous amine solutions, tertiary amine TEA proved to be the best-performing candidate with highest formate yield. The reason for the superior formate yield in TEA solutions was attributed to the presence of HCO_3^- as the solo CO_2 absorption product since HCO_3^- is more favorable to the hydrogenation process compared with carbamate species. As for the MEA and DEA solutions, the CO_2-capturing products mainly included HCO_3^- and carbamate species. The carbamate species was assumed to be hydrogenated via the HCO_3^- pathway as it can transform into HCO_3^- through equilibrium. The small mean particle size of 2.8 nm with a high content of Pd^0 on the surface of the catalyst and abundant amount of surface N-containing groups are the main reasons for the decent catalytic performance in the integrated CO_2 capture and hydrogenation process in the presence of the Pd/NAC catalyst. Finally, the reaction mechanism of integrated CO_2 capture and hydrogenation in aqueous amine solutions in the presence of Pd/NAC catalyst was proposed. The reusability, Pd leaching test and other physical–chemical characterizations of catalysts after the reaction are within the research scope of our plans to further advance the integrated CO_2 capture and hydrogenation process to large scales.

Supplementary Materials: The following supporting information can be downloaded at: https://www.mdpi.com/article/10.3390/catal12080925/s1, Figure S1: XPS spectra of Pd 3d core level of the used Pd/NAC catalyst.

Author Contributions: Conceptualization, L.L.; methodology, C.Y.; investigation, X.C.; resources, M.X.; data curation, X.C.; writing—original draft preparation, L.L.; writing—review and editing, M.X. All authors have read and agreed to the published version of the manuscript.

Funding: This research was funded by THE FUNDAMENTAL RESEARCH FUNDS FOR THE CENTRAL UNIVERSITIES, grant number CXZX2021A02.

Data Availability Statement: The data that support the findings of this study are available from the corresponding author (Li, L.), upon reasonable request.

Acknowledgments: The work was financially supported by Technology Innovation Center for Land Spatial Eco-restoration in Metropolitan Area, Ministry of Natural Resources.

Conflicts of Interest: The authors declare no conflict of interest.

References

1. Chen, M.; Ma, Y.; Zhou, Y.; Liu, C.; Qin, Y.; Fang, Y.; Guan, G.; Li, X.; Zhang, Z.; Wang, T. Influence of Transition Metal on the Hydrogen Evolution Reaction over Nano-Molybdenum-Carbide Catalyst. *Catalysts* **2018**, *8*, 294. [CrossRef]
2. Wang, Y.; Ren, B.; Ou, J.Z.; Xu, K.; Yang, C.; Li, Y.; Zhang, H. Engineering two-dimensional metal oxides and chalcogenides for enhanced electro- and photocatalysis. *Sci. Bull.* **2021**, *66*, 1228–1252. [CrossRef]
3. Gao, R.; Deng, M.; Yan, Q.; Fang, Z.; Li, L.; Shen, H.; Chen, Z. Structural Variations of Metal Oxide-Based Electrocatalysts for Oxygen Evolution Reaction. *Small Methods* **2021**, *5*, 2100834. [CrossRef]
4. Zeng, H.; Xing, B.; Cao, Y.; Xu, B.; Hou, L.; Guo, H.; Cheng, S.; Huang, G.; Zhang, C.; Sun, Q. Insight into the microstructural evolution of anthracite during carbonization-graphitization process from the perspective of materialization. *Int. J. Min. Sci. Technol.* **2022**. [CrossRef]
5. Li, L.; Conway, W.; Burns, R.; Maeder, M.; Puxty, G.; Clifford, S.; Yu, H. Investigation of metal ion additives on the suppression of ammonia loss and CO_2 absorption kinetics of aqueous ammonia-based CO_2 capture. *Int. J. Greenh. Gas Control* **2017**, *56*, 165–172. [CrossRef]
6. Rochelle, G.T. Amine Scrubbing for CO_2 Capture. *Science* **2009**, *325*, 1652–1654. [CrossRef] [PubMed]
7. Li, L.; Conway, W.; Puxty, G.; Burns, R.; Clifford, S.; Maeder, M.; Yu, H. The effect of piperazine (PZ) on CO_2 absorption kinetics into aqueous ammonia solutions at 25.0 °C. *Int. J. Greenhouse Gas. Control* **2015**, *36*, 135–143. [CrossRef]
8. Li, L.; Chen, X.; Chen, Z.; Gao, R.; Yu, H.; Yuan, T.; Liu, Z.; Maeder, M. Heterogeneous catalysts for the hydrogenation of amine/alkali hydroxide solvent captured CO 2 to formate: A review. *Greenh. Gases Sci. Technol.* **2021**, *11*, 807–823. [CrossRef]
9. Li, Y.-N.; He, L.-N.; Liu, A.-H.; Lang, X.-D.; Yang, Z.-Z.; Yu, B.; Luan, C.-R. In situ hydrogenation of captured CO_2 to formate with polyethyleneimine and Rh/monophosphine system. *Green Chem.* **2013**, *15*, 2825–2829. [CrossRef]
10. McNamara, N.D.; Hicks, J.C. CO_2 Capture and Conversion with a Multifunctional Polyethyleneimine-Tethered Iminophosphine Iridium Catalyst/Adsorbent. *ChemSusChem* **2014**, *10*, 1114–1124. [CrossRef]
11. Guan, C.; Pan, Y.; Ang, E.P.L.; Hu, J.; Yao, C.; Huang, M.H.; Li, H.; Lai, Z.; Huang, K.-W. Conversion of CO_2 from air into formate using amines and phosphorus-nitrogen PN_3P-Ru(ii) pincer complexes. *Green Chem.* **2018**, *20*, 4201–4205. [CrossRef]
12. Lu, M.; Zhang, J.; Yao, Y.; Sun, J.; Wang, Y.; Lin, H. Renewable energy storage via efficient reversible hydrogenation of piperidine captured CO_2. *Green Chem.* **2018**, *20*, 4292–4298. [CrossRef]
13. González, E.; Marchant, C.; Sepúlveda, C.; García, R.; Ghampson, I.; Escalona, N.; García-Fierro, J.L. Hydrogenation of sodium hydrogen carbonate in aqueous phase using metal/activated carbon catalysts. *Appl. Catal. B Environ.* **2018**, *224*, 368–375. [CrossRef]
14. Stalder, C.J.; Chao, S.; Summers, D.P.; Wrighton, M.S. Supported palladium catalysts for the reduction of sodium bicarbonate to sodium formate in aqueous solution at room temperature and one atmosphere of hydrogen. *J. Am. Chem. Soc.* **1983**, *105*, 6318–6320. [CrossRef]
15. Su, J.; Yang, L.; Lu, M.; Lin, H. Highly Efficient Hydrogen Storage System Based on Ammonium Bicarbonate/Formate Redox Equilibrium over Palladium Nanocatalysts. *ChemSusChem* **2015**, *8*, 813–816. [CrossRef]
16. Bi, Q.-Y.; Lin, J.-D.; Liu, Y.-M.; Du, X.-L.; Wang, J.-Q.; He, H.-Y.; Cao, Y. An Aqueous Rechargeable Formate-Based Hydrogen Battery Driven by Heterogeneous Pd Catalysis. *Angew. Chem. Int. Ed.* **2014**, *53*, 13583–13587. [CrossRef] [PubMed]
17. Wang, F.; Xu, J.; Shao, X.; Su, X.; Huang, Y.; Zhang, T. Palladium on Nitrogen-Doped Mesoporous Carbon: A Bifunctional Catalyst for Formate-Based, Carbon-Neutral Hydrogen Storage. *ChemSusChem* **2016**, *9*, 246–251. [CrossRef]
18. Shao, X.; Xu, J.; Huang, Y.; Su, X.; Duan, H.; Wang, X.; Zhang, T. Pd@C3N4 nanocatalyst for highly efficient hydrogen storage system based on potassium bicarbonate/formate. *AIChE J.* **2016**, *62*, 2410–2418. [CrossRef]
19. Kar, S.; Goeppert, A.; Prakash, G.K.S. Integrated CO_2 Capture and Conversion to Formate and Methanol: Connecting Two Threads. *Accounts Chem. Res.* **2019**, *52*, 2892–2903. [CrossRef]
20. Plomp, A.J.; Vuori, H.; Krause, A.O.I.; de Jong, K.P.; Bitter, J.H. Particle size effects for carbon nanofiber supported platinum and ruthenium catalysts for the selective hydrogenation of cinnamaldehyde. *Appl. Catal. A Gen.* **2008**, *351*, 9–15. [CrossRef]
21. Kang, J.; Zhang, S.; Zhang, Q.; Wang, Y. Ruthenium Nanoparticles Supported on Carbon Nanotubes as Efficient Catalysts for Selective Conversion of Synthesis Gas to Diesel Fuel. *Angew. Chem. Int. Ed.* **2009**, *48*, 2565–2568. [CrossRef] [PubMed]
22. Lu, Y.; Jiang, Y.; Chen, W. PtPd porous nanorods with enhanced electrocatalytic activity and durability for oxygen reduction reaction. *Nano Energy* **2013**, *2*, 836–844. [CrossRef]

23. Chernov, A.N.; Astrakova, T.V.; Koltunov, K.Y.; Sobolev, V.I. Ethanol Dehydrogenation to Acetaldehyde over Co@N-Doped Carbon. *Catalysts* **2021**, *11*, 1411. [CrossRef]
24. Liu, J.; Ji, Y.-G.; Qiao, B.; Zhao, F.; Gao, H.; Chen, P.; An, Z.; Chen, X.; Chen, Y. N,S Co-Doped Carbon Nanofibers Derived from Bacterial Cellulose/Poly(Methylene blue) Hybrids: Efficient Electrocatalyst for Oxygen Reduction Reaction. *Catalysts* **2018**, *8*, 269. [CrossRef]
25. Arrigo, R.; Hävecker, M.; Schlögl, R.; Su, D.S. Dynamic surface rearrangement and thermal stability of nitrogen functional groups on carbon nanotubes. *Chem. Commun.* **2008**, *40*, 4891–4893. [CrossRef]
26. Arrigo, R.; Schuster, M.E.; Xie, Z.; Yi, Y.; Wowsnick, G.; Sun, L.L.; Hermann, K.E.; Friedrich, M.; Kast, P.; Hävecker, M.; et al. Nature of the N–Pd Interaction in Nitrogen-Doped Carbon Nanotube Catalysts. *ACS Catal.* **2015**, *5*, 2740–2753. [CrossRef]
27. Lee, J.H.; Ryu, J.; Kim, J.Y.; Nam, S.-W.; Han, mJ.H.; Lim, T.-H.; Gautam, S.K.; Chae, H.; Yoon, C.W. Carbon dioxide mediated, reversible chemical hydrogen storage using a Pd nanocatalyst supported on mesoporous graphitic carbon nitride. *J. Mater. Chem. A* **2014**, *2*, 9490–9495. [CrossRef]
28. Elek, J.; Nádasdi, L.; Papp, G.; Laurenczy, G.; Joó, F. Homogeneous hydrogenation of carbon dioxide and bicarbonate in aqueous solution catalyzed by water-soluble ruthenium(II) phosphine complexes. *Appl. Catal. A Gen.* **2003**, *255*, 59–67. [CrossRef]